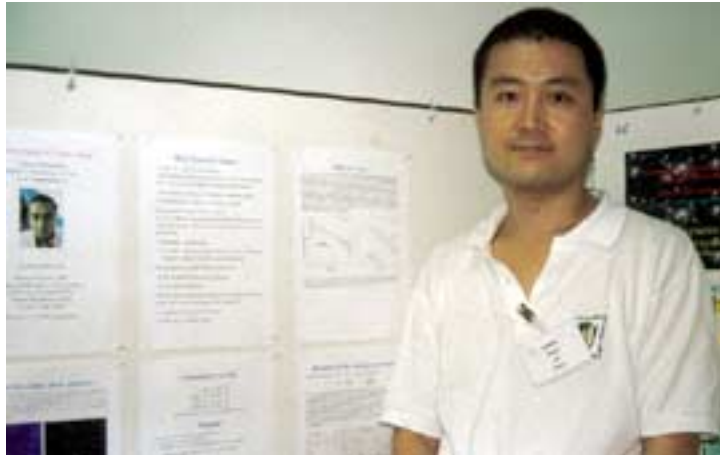


NUMERICAL STUDY OF THE COSMIC SHEAR



T. HAMANA¹, S. COLOMBI^{1,2}, and Y. MELLIER^{1,3}

¹ *Institut d'Astrophysique de Paris, CNRS, 98bis Boulevard Arago, 75014 PARIS, FRANCE*

² *NIC (Numerical Investigations in Cosmology) Group, CNRS*

³ *Observatoire de Paris, DEMIRM, 61 avenue de l'Observatoire, 75014 PARIS, FRANCE*

We study the cosmic shear statistics using the ray-tracing simulation combined with a set of large N -body simulations. We first describe our models and numerical method, and then present some selected results. We especially focus on; (1) effects of the deflection of light rays and the lens-lens coupling on the skewness of the lensing convergence which are neglected in making theoretical predictions of the cosmic shear statistics. (2) effects of the source clustering on a measurement of the skewness of the lensing convergence.

1 Introduction

The cosmic shear statistics have been known as a powerful tool for probing the large-scale structure formation as well as for placing the constraint on the cosmological parameters¹. Recently, four independent groups have reported the detection of the cosmic shear variance^{2,3,4,5}. Although those detections were done with relatively small fields which limit its accuracy, on going wide field cosmic shear surveys will provide a precious measurement of the cosmic shear variance as well as higher order statistics such like the skewness of the lensing convergence⁶.

Since the pioneering work by Gunn⁷, there has been a great progress in the theoretical study of the cosmic shear statistics⁸. The analytical formulae for computing the theoretical prediction of the cosmic shear statistics are based on the perturbation theory of the cosmic density field combined with the nonlinear clustering ansatz. Their accuracy and limitations should be tested against numerical simulations^{9,10}. Numerical simulations are also used to study the possible noises caused by, e.g., the cosmic variance and the clustering of sources as well as the clustering between sources and lenses (the, so-called, source clustering).

We study the cosmic shear statistics using the ray-tracing simulation combined with a set of large N -body simulations. Our study aims; (1) to test the theoretical predictions against the numerical simulations (2) to examine higher order statistics of the lensing convergence (3) to simulate the observation to examine the possible systematic effects, e.g., the source clustering. In this contribution, we first describe, briefly, our models and methods of numerical simulations. Then, we present some selected results, details are presented in¹¹.

Table 1: Parameters in three cluster normalized CDM Models

	Ω_m	Ω_λ	σ_8	h
SCDM	1.0	0.0	0.6	0.5
OCDM	0.3	0.0	0.85	0.7
Λ CDM	0.3	0.7	0.9	0.7

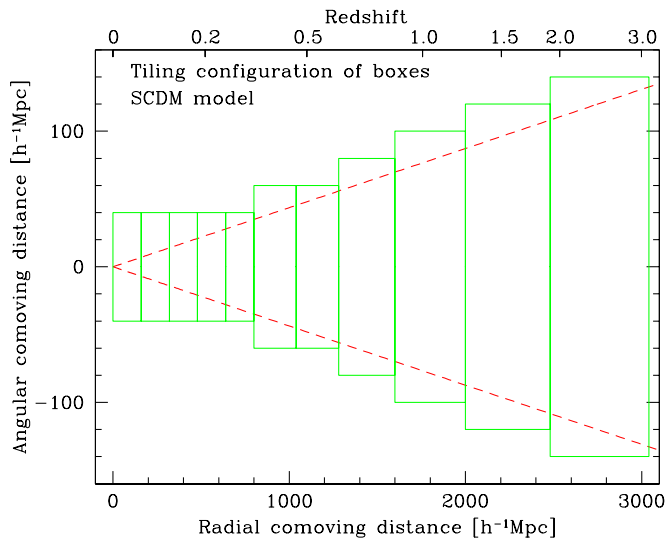


Figure 1: Tiling configuration of simulation boxes. Dashed lines shows the angular comoving distance of $\pm 2.5^\circ$.

2 Models and methods

We consider three cluster normalized cold dark matter (CDM) models, parameters in the models are summarized in Table 1. N -body simulations were performed with a vectorized particle-mesh (PM) code. They use $256^2 \times 512$ particles and the same number of force mesh in a periodic rectangular comoving box and use the light-cone output^{11,12}. In order to generate the density field from $z = 0$ to $z \sim 3$, we performed 11, 12 and 13 independent simulations for SCDM, OCDM and Λ CDM model, respectively. We adopted the *tiling* configuration of the boxes¹⁰, i.e., the box size of each realization is chosen so that we have a field of view of 5×5 square degrees (see Figure 1).

Light ray trajectories are followed through the density field generated by N -body simulations. The multiple lens-plane algorithm was used for the ray-tracing¹³. The lens planes (which are, at the same time, source planes) are located between $z = 0$ and $z \sim 3$ at intervals of $80h^{-1}\text{Mpc}$. For each ray, position of the ray on each lens plane is computed, and then the lensing magnification matrix, M_{ij} , is computed at the ray position on each plane. The lensing convergence, shear and net rotation are expressed by $\kappa = (M_{11} + M_{22})/2$, $\gamma_1 = (M_{11} - M_{22})/2$, $\gamma_2 = (M_{12} + M_{21})/2$, and $\omega = (M_{12} - M_{21})/2$, respectively. We performed 40 realizations for each model changing the underlying density field (i.e., making random shifts of boxes to x and y directions (perpendicular to the line-of-sight) using the periodic boundary condition in N -body simulations). For each realization, 512^2 rays are traced backward from the observer point. The initial ray directions are set on 512^2 grids with the grid spacing of $5^\circ/512 \sim 0.59$ arcmin.

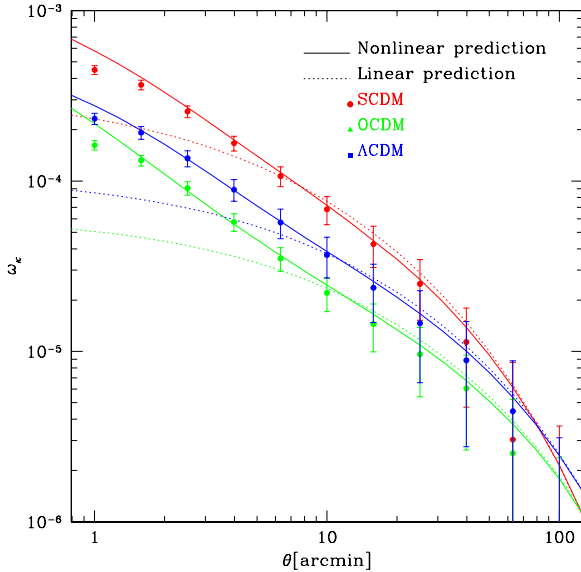


Figure 2: Two-point correlation functions of the lensing convergence. Sources are assumed to be a single redshift of $z_s \sim 1$.

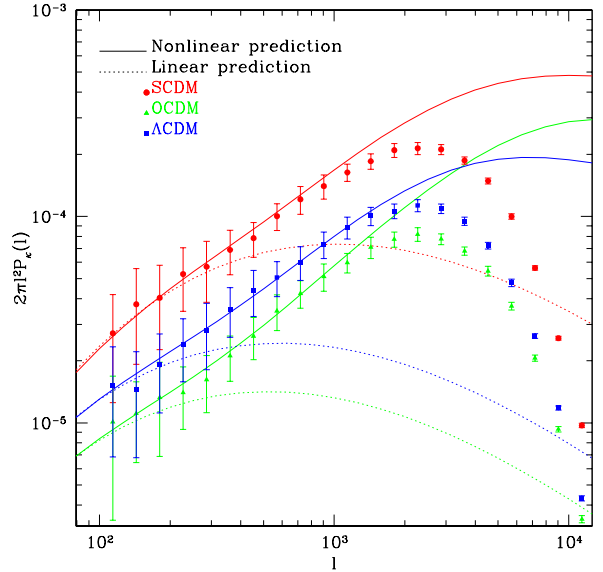


Figure 3: Power spectra of the lensing convergence. $l = 2\pi/\theta \sim 2.16 \times 10^4/\theta(\text{arcmin})$. Sources are assumed to be a single redshift of $z_s \sim 1$.

3 Results and discussion

3.1 Numerical resolution

Figure 2 shows the two-point correlations functions of the lensing convergence for three models compared with the linear (dotted lines) and nonlinear (solid lines) predictions¹⁴. Results of the ray-tracing simulations agree with the nonlinear predictions on scales between 2 arcmin and 50 arcmin. The loss of the power on large scales is a result of the lack of powers on scales larger than N -body simulation boxes. While the small scale resolution limit comes from the resolution of the N -body simulations. The spatial resolution of our PM N -body simulation is simply $\Delta x = L_{\text{box}}/256$. The angular resolution is limited by the angle subtended to Δx , i.e., $\Delta\theta \sim \Delta x/D_A(z)$, where $D_A(z)$ denotes the comoving angular diameter distance. Since we determined the box size so that the tiled set of boxes yields the field-of-view of 5×5 square degrees except boxes at very lower redshifts (see Figure 1), the angular resolution is roughly estimated by $5\text{degree}/256 \sim 1.2\text{arcmin}$. The discrepancy between this estimation and the angular scales of the saturation of the convergence two-point correlation function found in Figure 2 (about 2 arcmin) may be accounted by bad angular resolution at lower redshifts.

Figure 3 shows the power spectrum of the lensing convergence for three models compared with the linear (dotted lines) and nonlinear (solid lines) predictions¹⁴. Since $l = 2\pi/\theta \sim 2.16 \times 10^4/\theta(\text{arcmin})$, one may expect from the angular resolution found in the two-point correlation functions that the results of the ray-tracing simulations should agree with nonlinear prediction up to $l \sim 10^4$. The discrepancy between this expectation and the scale where the measurements start roll-off ($l \sim 10^3$) is due to the smoothing effect in the Fourier transformation using grids. In our case, it is estimated that the measurements start to deviate from the nonlinear prediction at a scale smaller about 0.1-0.2 times than the true scale. It is, therefore, said that our ray-tracing simulation combined with the tiled set of large PM N -body simulations yields the angular resolution of $\theta \sim 2$ or $l \sim 10^5$ for a source redshift of $z_s = 1$. It is important to note that the angular resolution varies with the source redshift, the resolution becomes better (worse) with increasing (decreasing) the source redshift.

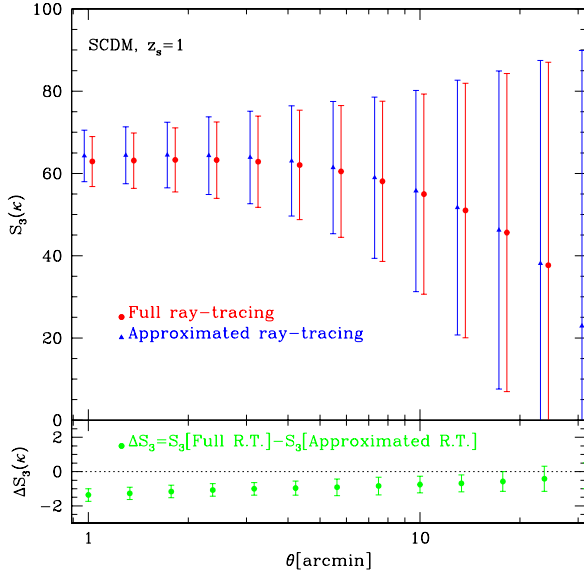


Figure 4: S_3 (upper panels) and ΔS_3 (lower panels) as a function of the smoothing angle θ_0 . Comparison of the skewness parameter S_3 computed from the results of *full* and *approximated* ray-tracing simulations (see text for details). Sources are assumed to be a single redshift of $z_s \sim 1$.

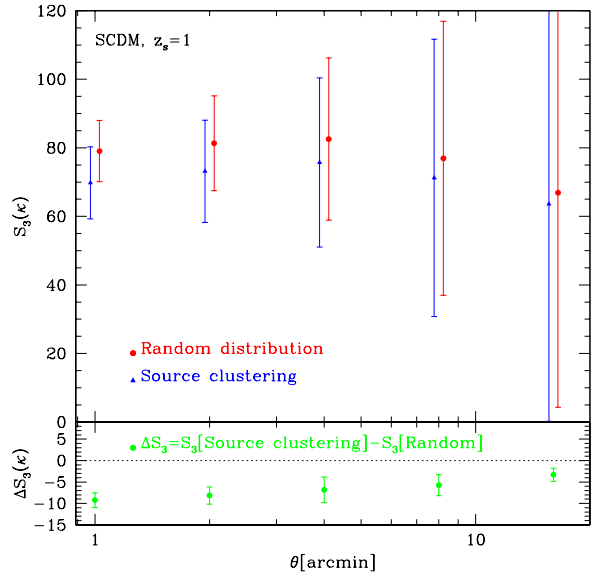


Figure 5: S_3 (upper panels) and ΔS_3 (lower panels) as a function of the smoothing angle θ_0 . Comparison of the skewness parameter S_3 computed from the results of the ray-tracing simulations with and without source clustering (see text for details).

3.2 Effects of neglecting the lens-lens couplings and of the Born approximation on the skewness of the lensing convergence

The theoretical predictions of the cosmic shear statistics have been made based on the perturbation theory approach in which the moments of the lensing convergence are calculated from a perturbative expansion of the density contrast¹⁶. In this approach, the linear order term of the convergence, $\kappa^{(1)}$ only arises from the linear order density contrast, $\delta_{\text{mass}}^{(1)}$. Note that the deflection of the light ray trajectory is neglected in computation of $\kappa^{(1)}$, this is the, so-called, *Born approximation*^{16,17}. The second order term arises not only $\delta_{\text{mass}}^{(2)}$ but also both the coupling between the lenses located at different redshifts, the, so-called, *lens-lens coupling* and the deflection of the ray trajectory. The latter two are usually neglected in computation of the skewness as well as the variance of the lensing convergence. For the computation of the variance, it is known that those two effects are safely neglected^{9,16}. Bernardeau et al.¹⁶ examined the effects of those two terms on the convergence skewness using the linear and quasi-linear theory and found that they are sufficiently small and can be neglected safely. There is, however, a priori no reason to believe that dropping the lens-lens coupling terms and the Born approximation are still correct in the non-linear regime.

We examined numerically the effects of neglecting the lens-lens couplings and of the Born approximation on the skewness of the lensing convergence. In addition to the usual *full* ray-tracing, we also performed the *approximated* ray-tracing, that is, the deflection of light rays and all lens-lens coupling terms are neglected in the ray-tracing simulations. From the results of those two kinds of ray-tracing, we compute the skewness parameter defined by $S_3 = \langle \kappa^3 \rangle / \langle \kappa^2 \rangle^2$ ¹⁶. Results are shown in Figure 4. It is clear from Figure 4 that neglecting the lens-lens couplings and of the Born approximation on the skewness of the lensing convergence has no significant effect. Although we only display a case for $z_s = 1$ in SCDM model, we found the similar results for other cosmological models and for other source redshifts¹¹. van Waerbeke et al.¹⁵ computed the effects of lens-lens couplings and Born approximation using the semi-analytic approach and

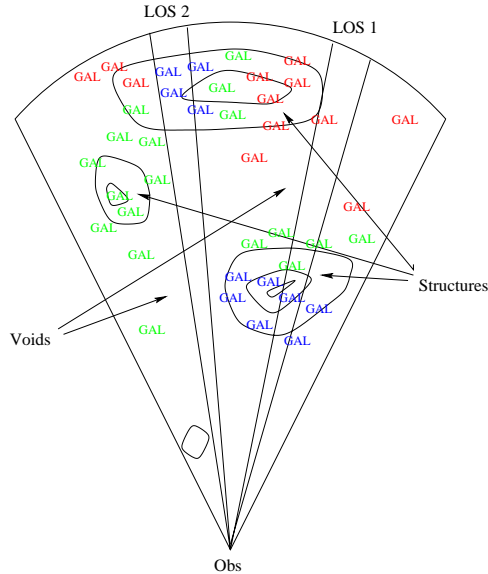


Figure 6: An illustration of the correlation between the lensing potential (contour lines) and the population of sources (denoted by symbols “GAL”).

found a good agreement between the numerical results and the semi-analytic predictions.

3.3 Source clustering effect on the skewness of the lensing convergence

Bernardeau¹⁸ pointed out that the correlation between the source galaxies and the lensing potential reduces the amplitude of the skewness and showed that the effect is sensitive to the redshift distribution of sources. The source clustering effects result from three facts, namely, (1) The source galaxies are not randomly distributed in the sky but are correlated. (2) The distribution of the source galaxies traces somehow the matter field. (3) The redshift distribution of source galaxies is rather broad and its width depends on a criterion of the source selection. Consequently, distribution of source galaxies is overlapped with the distribution of lensing structures, and thus the source galaxies are correlated somehow with the lensing potential. This correlation causes systematic effects on measurements of the cosmic shear, that may be illustrated as follows; Figure 6 shows, for example, the distribution of sources (denoted by symbols “GAL”) and the lensing potential (contour lines). For a line-of-sight 1 (LOS 1), the distant galaxies are lensed by the lensing potential located at intermediate distance and thus have the high *positive* lensing signal. This high signal is reduced by the excess of the foreground sources which correlated with the foreground lensing potential and have a low lensing signal. While for a line-of-sight 2 (LOS 2), the distant sources are lensed by the foreground void and thus have a *negative* lensing signal. This negative signal is emphasized because of the lack of foreground sources in the void. Accordingly, the probability distribution function of the lensing signal, i.e. the lensing convergence, modified, typically becomes more symmetric than that of the case of a random distribution of source galaxies. As a result, the amplitude of skewness of the lensing convergence drops.

We examine effects of the source clustering effect using a toy model of the galaxy distribution combined with the ray-tracing simulation. We adopt the canonical parametric model of the redshift distribution of source galaxies; $n_s(z) \propto (z/z_*)^\alpha \exp[-(z/z_*)^\beta]$. The distribution of the sources are chosen so that it linearly follows the underlying dark matter distribution in which the ray-tracing simulations were done, i.e., $\delta_{\text{gal}} \propto \delta_{\text{mass}}$, accordingly there is no bias between the distribution of the matter and galaxies. For each galaxy, we assign the lensing signals, lensing convergence and shear, by interpolating them from four closest ray positions on the nearest

source plane. Then we average the lensing convergences over sources located within an angular radius, θ_0 , that is, we compute the top-hat filtered lensing convergences. It should be noted that we did not take the intrinsic ellipticity of the galaxies into account. We also generate the random distribution of source galaxies. In this case, the sources have the same redshift distribution as the clustering case, but the angular distribution is random. Accordingly there is no source clustering effect in this case. We also compute the the top-hat filtered lensing convergences for the random distribution case in the same way as the above.

The results are shown in Figure 5 in which the parameters in the redshift distribution of sources are chosen by $\alpha = 3$, $\beta = 1.8$ and $z_* = 0.67$. Figure 5 indicate that the source clustering have a non-negligible effects on a measurement of the convergence skewness.

We examined the source clustering in detail using more realistic models of the galaxy distributions and also using the semi-analytic approach¹⁹. We found that the source clustering reduces the skewness about 10 percents for a realistic model of the redshift distribution of the sources and also found that the effect strongly depends on the bias. We also found that the source clustering effect can be reduced below a few percents by (1) going to a deep magnitude to increase the mean source redshift and (2) using only fainter images to reduce the width of the distribution of source galaxies.

Acknowledgments

We would like to thank L. van Waerbeke, F. Bernardeau and A. Thion for fruitful discussions. This research was supported in part by the Direction de la Recherche du Ministère Français de la Recherche. The computational means (CRAY-98) to do the N -body simulations were made available to us thanks to the scientific council of the Institut du Développement et des Ressources en Informatique Scientifique (IDRIS) Numerical computation in this work was partly carried out at the the TERAPIX data center. T.H. would like to thank the conference organization for financial supports.

References

1. Y. Mellier, ARAA, **37**, 127 (2000).
2. L. van Waerbeke et al., A&A, **358**, 30 (2000).
3. D. Bacon, A. Refregier and R. Ellis, MNRAS submitted (astro-ph/0003008), (2000).
4. D. N. Wittman et al., Nature, **405**, 143 (2000).
5. N. Kaiser, G. Wilson and G. A. Luppino, ApJ submitted (astro-ph/0003338), (2000).
6. DESCART project, <http://terapix.iap/Descart/>.
7. J. E. Gunn, ApJ, **150**, 737 (1967).
8. M. Bartelmann and P. Schneider, submitted to Physics Report (astro-ph/9912508), (2000)
9. B. Jain, U. Seljak and S. White, ApJ, **530**, 547 (2000).
10. M. White and W. Hu, ApJ, **537**, 1 (2000).
11. T. Hamana, S. Colombi and Y. Mellier, in preparation, (2000).
12. T. Hamana, S. Colombi and Y. Suto, A&A submitted (2000).
13. P. Schneider, J. Ehlers, & C. C. Falco, *Gravitational Lenses* (Springer, Berlin, 1992).
14. B. Jain and U. Seljak, ApJ, **484**, 560 (1997).
15. L. van Waerbeke et al., in preparation (2000).
16. F. Bernardeau, L. van Waerbeke and Y. Mellier, A&A, **323**, 1 (1997).
17. P. Schneider, L. van Waerbeke, B. Jain, and G. Kruse, MNRAS, **296**, 873 (1998)
18. Bernardeau, F. 1998, A&A, 338, 375 (B98)
19. T. Hamana, et al., in preparation, (2000).